Structures 71 (2025) 107892

Contents lists available at ScienceDirect

Structures

journal homepage: www.elsevier.com/locate/structures

Development and performance evaluation of an auxetic yield metal damper for enhanced seismic energy dissipation

Mehrdad Ashtari [a], Saeed Lari [b], Hakan Çağlar [c], Majid Pouraminian [d], Rohollah Salmani [e], Ahmed Genjaly [e,*]

[a] Department of Mechanical Engineering and Materials Science, University of Pittsburgh, Benedum Hall, 3700, O'Hara Street, Pittsburgh, PA 15261, USA
[b] Department of Civil Engineering, Eshragh Institute of Higher Education, Bojnourd, Iran
[c] Faculty of Engineering and Architecture, Department of Civil Engineering, Kırşehir Ahi Evran University, Kırşehir, Turkey
[d] Department of Civil Engineering, Ramsar Branch, Islamic Azad University, Ramsar, Iran
[e] Department of Mechanical Engineering, Tabriz University, Tabriz, Iran

ARTICLE INFO

Keywords:
Auxetic damper
Yield metal damper
Energy dissipation
Ductility
Nonlinear finite element

ABSTRACT

In this study, a new auxetic yield metal (AYM) damper is introduced for the first time based on the application of the auxetic structure. The performance of the proposed system is investigated via nonlinear finite element analysis by using ABAQUS commercial code. These types of steel dampers are fabricated from mild steel plate with elliptical holes and dissipate energy through the inelastic deformation of the constitutive material. To assess the capability of the proposed AYM damper, a set of nonlinear quasi-static finite element analyzes has been conducted on the damper with various geometric parameters. To ensure that the numerical models accurately predict the responses of AYM dampers, experimental validation techniques were employed. This validation confirms the models' sufficient accuracy in representing the dampers' behavior. According to the results, the proposed AYM damper exhibits a low yield displacement, stable hysteretic loops, a good range of ductility, and a high energy dissipating capacity. The specific energy absorption and ductility of the proposed auxetic damper are 32.5 J/kg and 59, respectively. With its ductile behavior, this damper can dissipate a large amount of earthquake input energy. Furthermore, it is found that the use of proposed auxetic dampers in the steel frame, increases the hardness, strength and ductility of the frame and the energy absorption increased by 210 %.

1. Introduction

Nowadays, passive energy dissipation systems in structures are regarded as an effective and suitable method to reduce earthquake damages [1–4]. This energy dissipation can be based on various mechanisms, the most remarkable of which are inelastic deformations of ductile metal in metallic dampers, friction slip in frictional dampers, fluid passage through narrow holes in viscous dampers, and deformation in viscoelastic dampers [5].

One of the most prevalent and oldest passive control tools employed to control and reduce the seismic responses of structures under severe earthquakes are metallic yield dampers [6,7]. This type of dampers uses the feature of metal yield or the same hysterical behavior of metals when deformed in the plastic area, which increases the energy dissipation. Furthermore, these dampers increase the stiffness. Metallic yield dampers hold numerous forms, including central yield components, U-shaped components, and damping and hardening elements in the form of triangular sheets (TADAS) or X-shaped sheets. Mohammadi et al. [8] investigated the behavior of TADAS dampers using experimental tests and finite element modeling. The results of their study reveal that the force-displacement curve of the presented TADAS damper can be divided into four distinct areas. Using two welded tubes, Maleki and Mahjoubi [9] introduced a new damper to improve energy absorption. Chan and Albermani [10] investigated the use of steel slit dampers in vertical beams. The constructed samples were subjected to uniform and cyclic loading. Their experimental results showed two important properties of steel dampers that include a stable ability to dissipate energy as well as a suitable model for reciprocating behaviors. Balendra et al. [11] investigated a new hybrid system for operation at two different levels of force. This system consists of elbow brace and slotted bolted connection in series connected to both ends of the diagonal brace. Downey et al. [12] suggested a new friction system to reduce the seismic response of

* Corresponding author.
E-mail address: ahmed.genjaly@tabu.ac.ir (A. Genjaly).

https://doi.org/10.1016/j.istruc.2024.107892
Received 17 November 2022; Received in revised form 27 October 2024; Accepted 19 November 2024
Available online 2 December 2024

steel frames. Azandariani et al. [13] offered a new damper utilizing two steel rings and examined its performance using numerical and analytical solution methods. Guo et al. [14] designed a new metal damper applying steel strips. In their model, steel strips act as energy absorption and dissipation factor. In another study, Guo et al. [15] conducted experimental tests to investigate the performance of metal dampers consisting of X-shaped pipe dampers. Khosravi et al. [5] investigate the dynamic performance of a novel mechanical metamaterial developed for seismic isolation in multi-story buildings. This seismic isolator, termed the meta-isolator, leverages solid friction alongside inherent viscous damping to improve energy dissipation capabilities. Lu et al. [16] introduce a novel device, the lateral damping buffer, designed to enhance building resilience against debris flows. This lateral damping buffer employs two primary damage mitigation mechanisms: upon debris flow impact, it functions as a buffer to absorb the initial force, and as the structure vibrates from the impact, it serves as a shock absorber, effectively reducing both the peak acceleration response and subsequent vibrations. Zhao et al. [17] experimentally investigate the parameter sensitivity of the pounding tuned mass damper applied to a traffic signal structure. By analyzing the control of both free and forced vibrations across various harmonic frequencies, the study evaluates the damper sensitivity to parameter variations.

Over the last decades, remarkable advances in science and technology have prompted researchers to find new structural materials, such as materials with a negative Poisson's ratio (NPR). In dampers, an NPR structure can significantly enhance energy dissipation by undergoing large plastic deformations under both tensile and compressive forces. This is particularly advantageous in seismic applications, where structures experience cyclic loading and require dampers that can maintain stability and energy absorption over repeated cycles. The lateral expansion under tension also allows for better stress distribution across the damper, reducing the likelihood of premature failure and increasing the damper's overall lifespan. Additionally, the auxetic structure's resilience against buckling makes it well-suited for applications involving large displacements and high strain demands. This structural stability, combined with enhanced ductility, enables auxetic dampers to dissipate seismic energy effectively without compromising the damper's structural integrity. Therefore, incorporating NPR materials into damper design offers a promising approach to achieving high-performance seismic dampers capable of meeting the demands of earthquake-resistant structures. To date, many materials with this property have been discovered, fabricated, or proposed. These materials have unique properties that have been appealing for special applications.

In the 1800s, Lim et al. [18] discovered the properties of auxetic behavior in some materials. At the time, auxetic materials were confined to natural materials and were not paid much attention. Lakes [19] first presented a cellular configuration with auxetic properties that could be easily fabricated using a triple compression and heating method. Auxetic materials have recently seen rapid expansion and development within their field, largely due to their unique properties that make them suitable for a wide range of applications, including personal protection, military uses, medical devices, as well as in the textile and aerospace industries. Despite numerous proposed uses, practical applications of auxetic materials remain in the early stages. Therefore, ongoing efforts are essential to enhance and develop functional auxetic materials for broader implementation.

Auxetic materials exhibit unique properties compared to conventional materials, including reduced Young's modulus, enhanced shear modulus, increased impact resistance, dual curvature capabilities, improved fracture toughness and crack resistance, greater energy absorption, and adjustable permeability. Zhang et al. [20] reviewed studies of large deformation and energy absorption of NPR materials. Meena and Singamneni [21] recommended a novel auxetic construction to decrease the influence of stress attentiveness. Ren et al. [22] examined the performance of tubular auxetic configurations below tensile load. Their results indicate that if the regular constraints of the structure

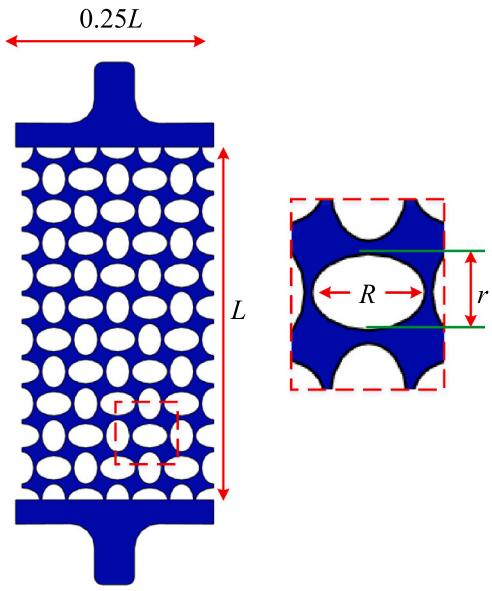

Fig. 1. Novel proposed AYM damper.

are selected properly, the mechanical properties of the designed auxetic structure can be substantially increased. Hassanin et al. [23] examined the perception conflict of auxetic configurations. Guo et al. [24] mathematically analyzed the mechanical performance of auxetic tubular constructions below compressive loading. Nedoushan [25] investigated the influence of size and cross-section of metal cylindrical-shaped configurations with NPR on their energy absorption characteristics, experimentally and finite element. The results of his study demonstrated that using structures with NPR with small cell size has more axial stability. Peixinho et al. [26] conducted an in-depth investigation into the compressive properties and energy absorption capabilities of metal-polymer hybrid cellular structures. They concluded that the mechanical performance of these metal-cell structures is significantly influenced by the intrinsic characteristics of the base material, as well as by the size, shape, and arrangement of the cells within the structure.

Reviewing previous work in this field indicates that although several models have been suggested for absorbing energy, damping structures with a NPR have not been adequately considered. Consequently, in this study, a numerical approach is suggested for the first time for determining the capability of auxetic materials to be used in yield dampers. For this purpose, a new three-dimensional auxetic structure has been proposed that can be fabricated from steel plates and has high stability and adjustable stiffness at the same time. An experimental validation technique was used to validate the numerical model, which was developed using commercial finite element software. Subsequently, after examining the influence of different geometric parameters on the energy absorption capacity of this new structure, its performance on a single-story steel frame has been numerically investigated.

2. Auxetic yield metal (AYM) damper

As evident, the properties of the base material and the topology of the cells control the mechanical properties of the cellular auxetic materials [27,28]. The energy absorption capacity of auxetic structures is way higher than conventional structures. Therefore, the damper presented in this research is an auxetic metallic yield damper that possesses the capacity to dissipate energy through plastic deformation. AYM damper, according to Fig. 1 comprises three main parts, including steel base plate, elliptical holes, and side fasteners. According to the figure, the steel base plate is rectangular with dimensions of$L \times 0.25L$. The large diameter and small diameter of the elliptical holes are equal to R and r, respectively. If the number of holes in the base plate is N, then the

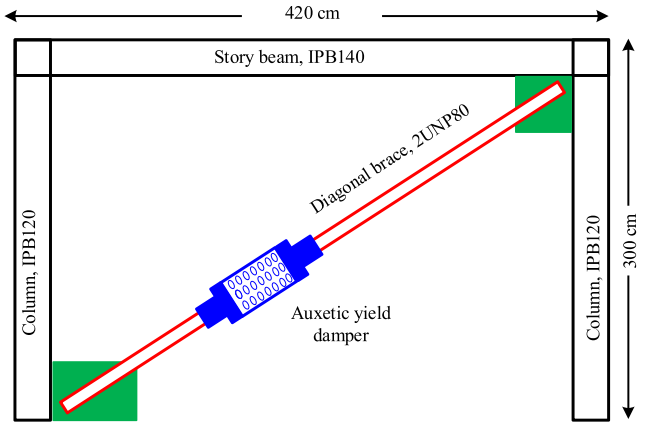

Fig. 2. Installation of the suggested AYM damper in a diagonally braced steel frame.

volume fraction of porosity can be calculated as follows:

$$\phi = 4NA/L^2 \tag{1}$$

where $A = \pi rR$ is the area of the elliptical holes. Therefore, the equivalent density of the auxetic structure can be calculated as follows:

$$\rho^*/\rho_s = 1 - \phi \tag{2}$$

where ρ^* is the equivalent density of the auxetic structure and ρ_s is the density of the steel plate. Hence, the four major parameters, including base sheet size L, small circle radius, r, and large radius, R, elliptical holes, as well as the volume fraction of porosity,ϕ, are influential in designing the new auxetic metal yield damper. Consequently, the energy absorption capacity of this damper will depend on these parameters, which will be taken into account over the course of this study. Total absorbed energy (E_a) is the energy absorbed by the structure during deformation to the final state of deformation, which can be acquired by integrating the force-displacement curve:

$$E_a(J) = U = \int_0^{\delta} F(\delta)d\delta \tag{3}$$

where δ represents the displacement.

In this research, so as to compare the energy absorption efficiency of structures with various densities, the concept of specific energy absorption is utilized. Specific absorbed energy (SEA) is defined as the energy absorbed by the structure's unit mass, which is the ratio of the total absorbed energy to the mass of the structure, W. Specific absorbed energy (SEA) obtained as:

$$SEA(J/kg) = \frac{E_a}{W} \tag{4}$$

The term "auxetic metallic yield damper" refers to a damper structure that leverages an auxetic (NPR) design to enhance energy dissipation and deformation capacity. This damper is engineered to withstand both tensile and compressive forces during seismic events, rather than experiencing only tensile forces. In seismic loading conditions, the structure naturally undergoes alternating tensile and compressive stresses due to oscillatory movements.

The auxetic design of the damper enables it to expand laterally under tension and contract uniformly under compression, which helps distribute stresses and reduces the likelihood of premature buckling. This behavior is particularly beneficial for seismic applications, as it allows the damper to absorb energy effectively in both loading directions. By sustaining large plastic deformations, the auxetic structure significantly enhances the damper's ability to dissipate energy under both tensile and compressive cycles.

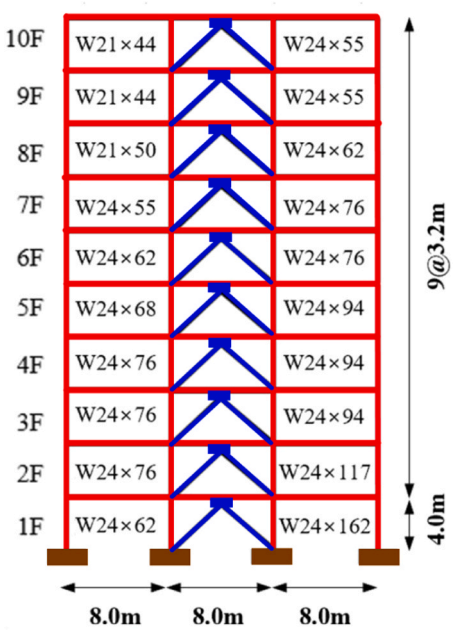

Fig. 3. The section properties of the damper brace configurations of 10-story steel bending frame model.

Moreover, the damper is positioned within an 8-shaped bracing system that efficiently channels seismic forces through the auxetic damper. This configuration ensures that the damper responds to cyclic loading without being limited to a single loading direction. The combined auxetic and bracing design allows the damper to capitalize on the natural bidirectional forces present during an earthquake, achieving consistent and reliable energy dissipation throughout seismic events.

3. Steel frame equipped with AYM damper

This paper presents a new passive damper system of combination of auxetic materials and metallic yield dampers for energy dissipation in steel frames, which is shown in the steel frame in Fig. 2. As illustrated in Fig. 2, the proposed AYM damper is located between the diagonal brace and the gusset plate connection. This damper can be connected to the diagonal brace using bolts or welded joints. One of the significant advantages of the seismic performance of this damper is its simple design and construction and its ease of installation and replacement in the bracing system. Since the suggested damper acts as a fuse and holds a nonlinear behavior as a ductile element, it has a heightened ability to absorb energy. Hence, in order to attain a proper function for this damper, its central core must be correctly designed to have high ductility and strength. Therefore, other structural components should be designed based on the load-bearing capacity of the structure to operate within the elastic range. In the proposed design, the AYM damper will act as a fuse element and energy absorber in the braced frame, and the effect of different parameters on its performance will be examined.

To estimate the performance of the proposed AYM damper in high-rise structures, a two-dimensional, 10-story steel bending frame model was developed. This model incorporates the newly designed metallic damper positioned within 8-shaped wind braces, as depicted in Fig. 3. The inter-story heights and bays width are set to 3.2 m and 8 m, respectively, while additional geometric, mechanical, and loading specifications, along with design parameters, are available in reference [29]. Seismic analysis of the structure equipped with the novel damper was performed using OpenSees software. Fiber beam-column elements were employed for the columns to accurately capture the interaction between axial force and bending moment. In this analysis, the behavior of all structural members, with the exception of the dampers, was

Table 1
Seismic records selected for nonlinear dynamic time history analysis.

Ground motion	Station	M	PGA (g)
Imperial Valley	H-E06230	6.5	0.44
Sanfernando 1971	PEL090	6.6	0.21
Tabas 1978	TAB-TR	7.4	0.85

assumed to remain elastic and linear. A multi-linear plastic link with kinematic hysteresis behavior is utilized to model the proposed damper, with force-displacement curves derived from numerical analysis results. The seismic records selected for the nonlinear dynamic time history analysis were all recorded on Type III soil, and detailed specifications for these records are provided in Table 1.

4. Nonlinear finite element modeling

Numerical methods like nonlinear finite element modeling represent advanced computational approaches used to analyze systems where nonlinear responses arise from material properties, boundary conditions, or loading conditions [30]. These methods are widely applied in engineering problems requiring detailed analysis of complex behaviors under various operational conditions [31–33]. In this section, the finite element analyses conducted on the AYM damper are presented, and the bracing system is examined. The ABAQUS finite element software is utilized to perform the analyses, and nonlinear static analysis is conducted by considering the tensile load for the auxetic metallic yield damper and the cyclic load for the braced system. Cyclic loading is applied to the braced frame to simulate seismic loads. The loading method is similar to the method proposed in the ATC-40 code, which is illustrated in Fig. 4a [34]. The boundary conditions and applied load are presented in Fig. 4b with the meshed samples. Three-dimensional elements of nonlinear 8-nodes have been utilized to mesh all the components understudy, and geometric nonlinearities and materials have been considered. The surface-to-surface contact algorithm with the normal property "Hard Contact" and the tangential behavior of "Penalty" method with a friction coefficient of 0.1 have been utilized to define the interaction between different surfaces of the damper. To simulate welded joints, Tie contact constraint has been deployed. To simulate the nonlinear behavior of steel materials, the material hardening is considered utilizing the isotropic-kinetic hardening model. Besides, the material of all components used in the analysis is assumed to be the same. Based on experiments, the stress-strain curve of steel is considered to be Trilinear material behavior, and the plasticity model is used based on the von-mises yield surface method [35]. For the elastic region, the elastic modulus and the Poisson's ratios are 200 GPa and 0.3, respectively. Moreover, the slope of the strain hardening zone is 2.4 GPa, and the yield stress of the steel used is 305 MPa [13].

Fixed boundary conditions were applied at the ends of the damper to replicate its attachment within the frame. The boundary setup prevented any rigid body motion while allowing for the natural deformation of the auxetic structure. Cyclic loading was applied to simulate seismic forces, with a displacement-controlled loading protocol that incrementally increased the displacement in tension and compression. This setup enabled the evaluation of energy dissipation and load-bearing behavior under repeated loading cycles. The finite element model of the auxetic metallic damper was constructed in ABAQUS, using 3D solid elements of type C3D8R, which are 8-node linear brick elements with reduced integration. This element type was selected due to its ability to effectively model the nonlinear behavior and complex deformation patterns of metallic structures under cyclic loading.

To ensure that the simulation results were not influenced by mesh

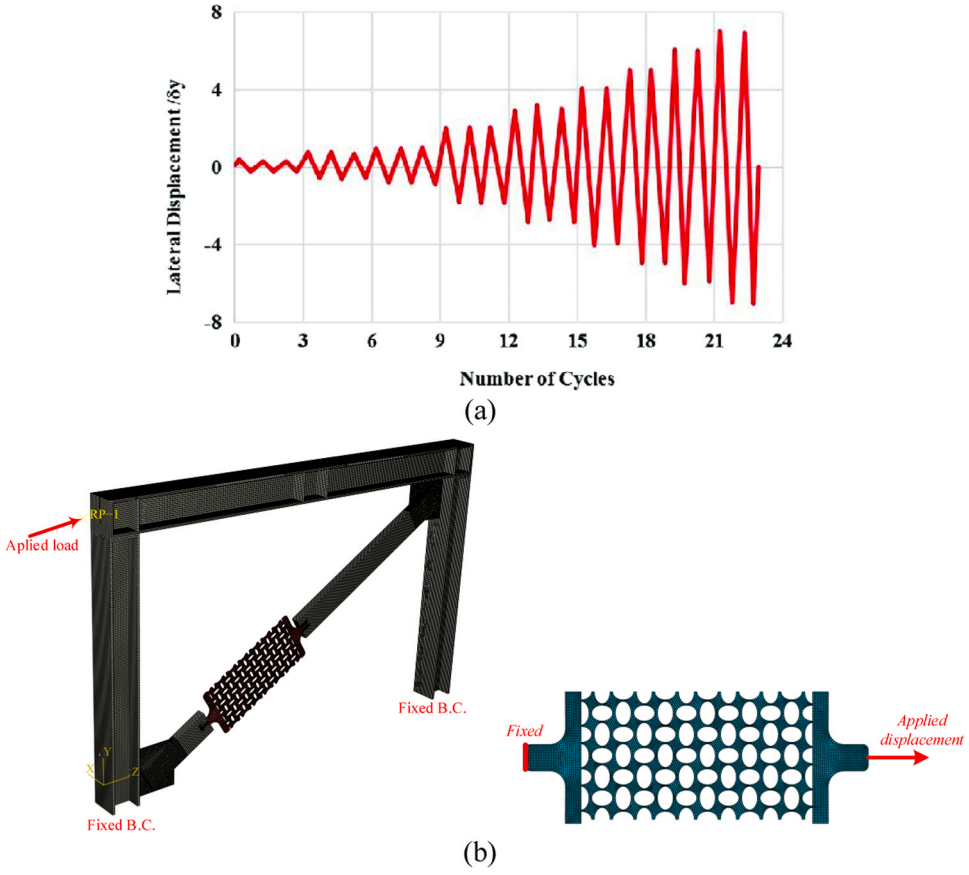

Fig. 4. (a) Cyclic loading based on the ATC24 protocol [35], and (b) Boundary conditions, loading, and meshing of the proposed damper assembled on the braced steel frame.

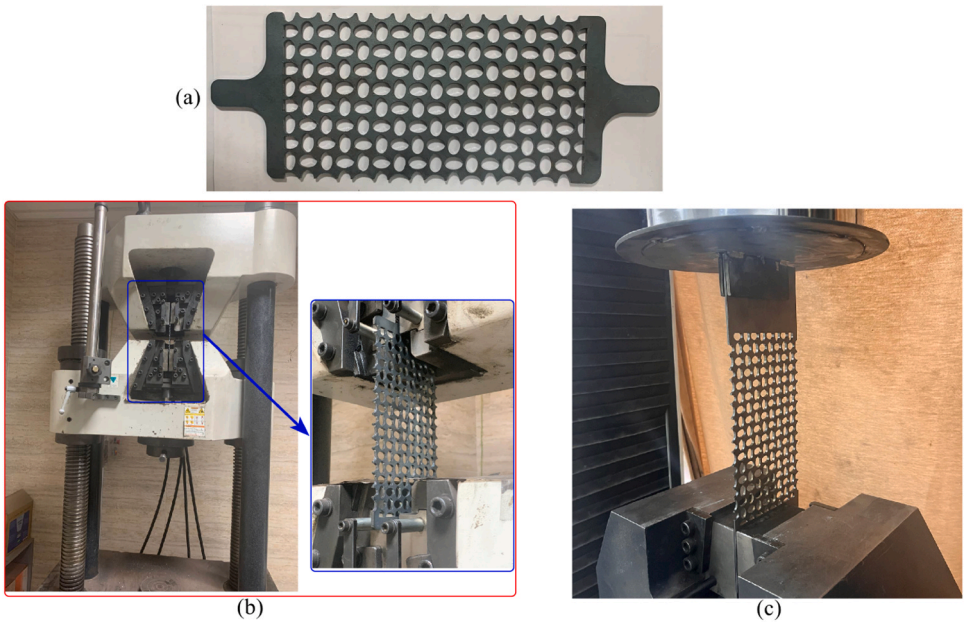

Fig. 5. (a) Side view of the manufactured auxetic yield damper, and experimental setup of uniaxial test for the manufactured specimen, (b) uniaxial tension and (c) uniaxial compression.

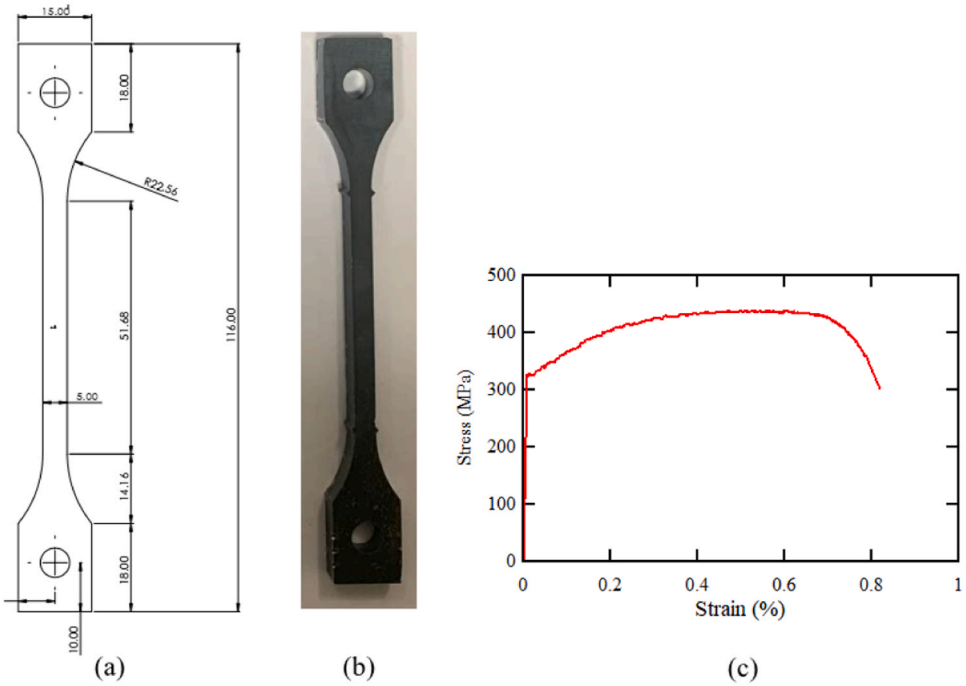

Fig. 6. (a) Tension coupons dimensions, (b) fabricated tension coupons, and (c) stress–strain curves obtained from the tensile test.

density, a mesh independence study was conducted. The model was initially meshed with coarse elements, and the mesh was progressively refined until changes in key output parameters—such as maximum displacement, yield strength, and energy dissipation—became negligible (less than 2 %). Based on this analysis, the optimal element size was determined to be 0.2 mm for areas near the auxetic holes where stress concentrations are highest and 0.5 mm for regions away from the holes. The final model consisted of approximately 320,000 C3D8R elements, with mesh refinement concentrated around the elliptical holes in the auxetic structure. This fine mesh ensured accurate stress and strain distribution, especially in regions undergoing large plastic deformations.

5. Experimental program

The proposed auxetic yield damper has been experimentally tested to verify the results of the finite element analysis and laboratory study. Firstly, the sample with $\phi = 0.18$ and $R/r = 1.9$ is prepared from a steel sheet with a thickness of 3 mm, as shown in Fig. 5(a). The damper is manufactured through the use of water jet cutting. The key purpose of using this technique of cutting is its high accuracy, which prevents the generation of residual stress. Using a 100 kN universal testing machine,

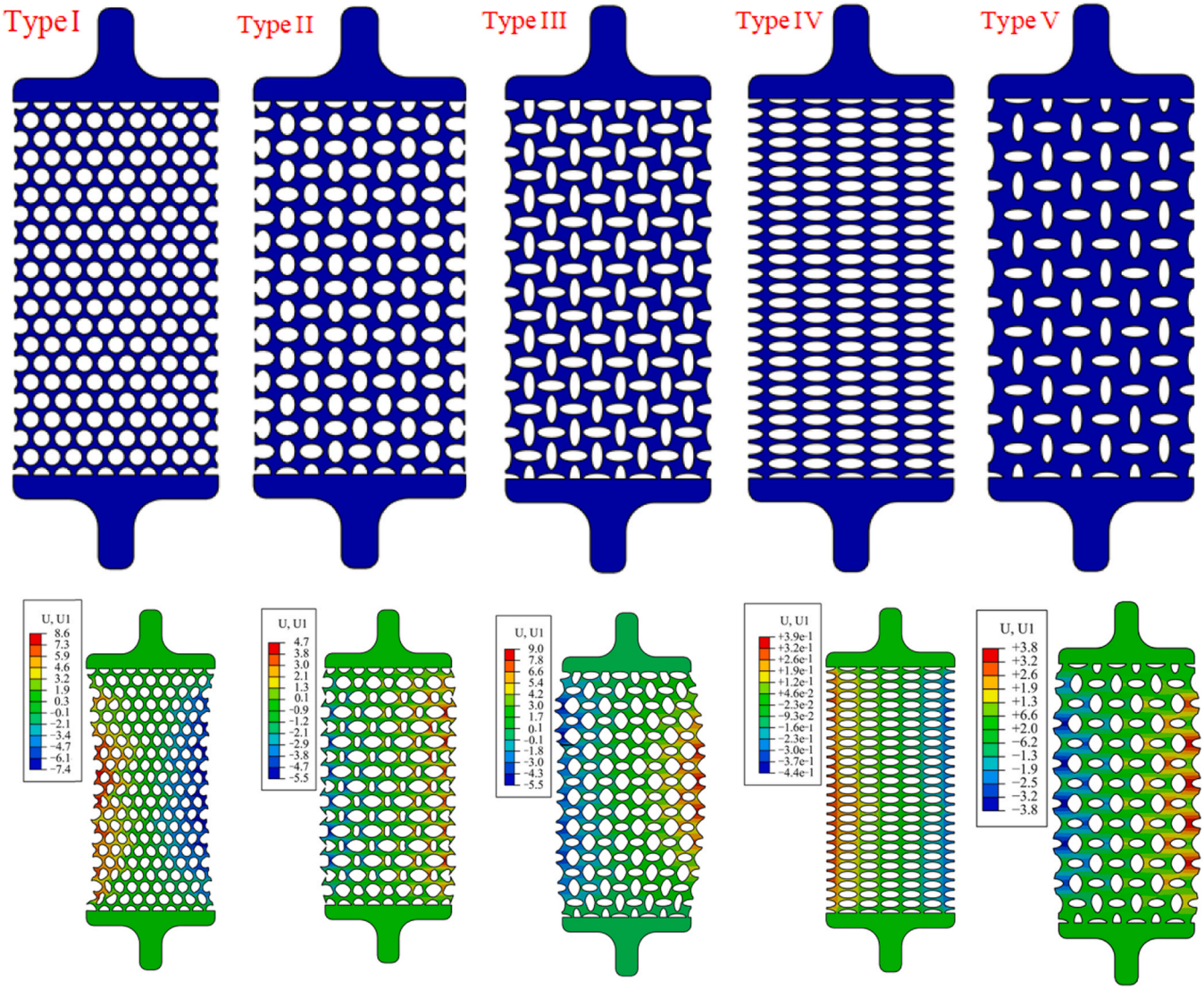

Fig. 7. Deformation mechanism (mm) of a number of different metallic damper samples presented for $R/r = 5/2,\ 3/2,\ 1,\ 1/2$, and considering the constant values of $L = 650$ ***mm*** and $\varphi = 0.140$ and the applied displacement of 2 cm.

tensile and compression tests were conducted to obtain the force-displacement curve for the damper. The experimental setup is illustrated in Figs. 5(b) and 5(c). The uniaxial compressive test was conducted using a servo-hydraulic press (INSTRON 5980) under displacement-controlled conditions at a constant rate of 0.5 mm/min. Both load and displacement measurements were recorded directly by the INSTRON 5980 system. The upper cross-head moves at a speed of 0.5 mm/min while the lower cross-head is fixed. To determine the mechanical properties of the auxetic yield damper material, tensile tests were conducted. A water jet machine was used to cut the tension coupons from the same material used in the construction of the auxetic yield damper. Fig. 6(a) shows the dimensions of the tensile coupons specimens as described in the ASTM E8M standard. In Fig. 6(c), the mean stress-strain response of steel coupon specimens is shown.

6. Results

In the current section, the results of finite element analyses conducted on the proposed auxetic yield damper and its performance on a diagonal braced steel frame sample are investigated. To that end, initially, the effect of geometric parameters, including the ratio of large diameter to small diameter of elliptical holes, R/r, volume fraction of holes,ϕ, and damper length, L, on the performance of the suggested damper is taken into consideration. Elastic stiffness (K_0), yield displacement (Δ_y), yield force (P_y), ductility ($\mu = \Delta_{max}/\Delta_y$), maximum load capacity (P_u) and specific energy absorption (SEA) have been selected as the parameters under consideration. The yield force is a substantial parameter in designing structures equipped with metallic dampers. If the yield force is overly high, the dampers may not slip in a moderate earthquake and the structure may act as a braced bending frame, causing damage to the structure. Furthermore, if this force is greater than the buckling of the braced member, in which the damper is placed, then the energy dissipated will be zero. The main reason is that no plastic change occurs in the damper. On the other hand, if the yield force is overly low, due to the weakness of the damper, the energy dissipation will be insignificant, and in this case, the frame will act like a bending frame. Between these two modes, the characteristics of the damper can be designed in such a way that the maximum amount of energy dissipation occurs. In that case, the optimal geometric characteristics for the damper are acquired. To meet that aim, in this section, initially, a parametric study is carried out on the performance of the suggested damper, and then the damper that owns the highest energy absorption and most desirable performance characteristics is determined. Eventually, the efficiency of this damper in a steel frame is

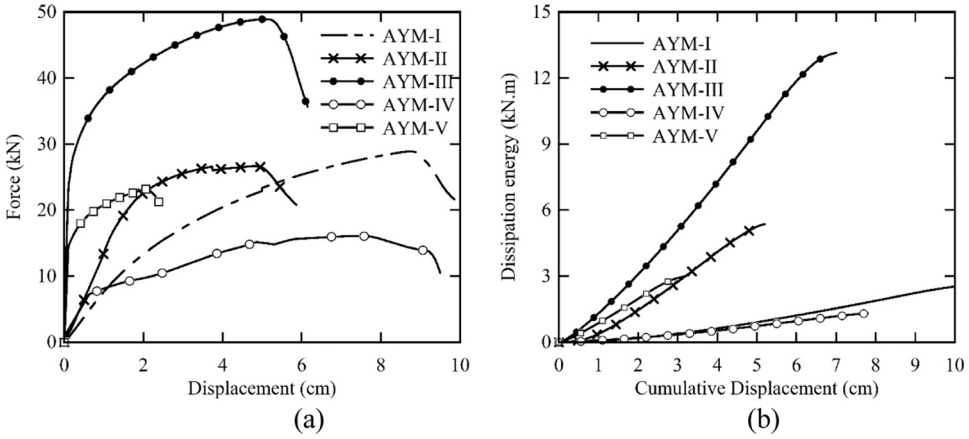

Fig. 8. (a) Load-displacement curve, and (b) Dissipation energy in AYD damper.

examined.

6.1. The performance of proposed auxetic yield damper

Fig. 7 demonstrates the deformation mechanism of a several different samples for $R/r = 5/2,\ 3/2,\ 1,\ 1/2$, and considering the constant values of $L = 650$ mm and $\varphi = 0.140$ and for constant displacement of 2 cm. According to the results, it can be inferred that the size of the holes and their distribution have an important influence on the deformation of this type of structure, and for some of the studied conditions, a NPR is generated. The behavior of samples with regular and uniform holes, i.e., samples I and IV, has a NPR and non-auxetic behavior. By applying tension, the middle part of the samples is reduced in length, and the amount of reduction in the length of the central area for these samples are 4.5 % and 0.24 %, respectively. Furthermore, the increase in the length of the central area for samples II, III and V, which have auxetic behavior, is equal to 2.9 %, 4.4 % and 2.1 %, respectively. Considering these results, it can be concluded that increasing the volume fraction of holes, and also utilizing elliptical holes with non-uniform distribution increases the auxetic behavior of the structure. Hence, the sample III has the best behavior. Additionally, a comparison of the deformations of samples III and IV, which have the same porosity volume fraction and holes of equal size (equal R/r ratio), demonstrates that changes in the distribution of holes can affect the behavior of the structure. Structure of type III, in which the elliptical holes are placed horizontally and vertically on the steel plate, has an auxetic behavior and will have many deformations compared to structure IV, which has a positive Poisson behavior, resulting in high energy absorption.

In order to analyze the influence of various parameters on the performance of the new damper, the load-displacement curve for the different samples illustrated in Fig. 7 are presented in Fig. 8a. According to the figure, it can be observed that samples III and V have more stiffness and initial strength than other samples. However, their strength decreases substantially after maximum capacity and proceeds with a negative slope. Moreover, the results show that the yield force for samples I, II, III, IV and V is 8.9 KN, 15.1 kN, 22.2 kN, 5.1 kN and 15.1 kN, respectively. Therefore, it can be stated that among the various samples under study, the auxetic AYD-III sample has the highest yield force and will be suitable to use as a damper.

Fig. 8b reveals the energy dissipation by the plastic deformation of the AYD damper in terms of the displacement. Considering the results, it is concluded that the energy dissipation due to plastic yield and plastic deformation has the lowest value for sample IV, and the auxetic sample AYD-III has a high energy dissipation capacity. This curve clearly demonstrates the high ability of auxetic structures to dissipate energy. In addition, for this sample, as can be observed, more resistance rate is seen for displacements more significant than 5 cm. This phenomenon, in addition to the impacts of strain stiffness, is due to the several deformations and increasing geometric nonlinearity in auxetic samples.

Table 2
Initial stiffness, yield displacement, yield strength, maximum ductility, maximum load capacity, and energy dissipation of auxetic damper samples.

	K_0 (kN/cm)	F_y (kN)	Δ_y (mm)	F_u (kN)	Δ_{max} (cm)	Ductility	SEA (J/kg)
AYD-I	6.56	8.96	13.3	28.6	8.8	7.98	211.4
AYD-II	18.68	15.16	9.8	26.2	4.7	4.67	122.1
AYD-III	143.34	22.25	1.4	48.9	5.1	64.02	261.2
AYD-IV	44.87	5.06	1.9	16.1	7.4	49.28	108.5
AYD-V	132.35	15.13	1.6	23.2	2.1	18.46	48.6

Based on the results presented in Fig. 8a, the parameters of initial stiffness, yield displacement, yield strength, maximum ductility, maximum load capacity and energy dissipation of the samples are given in Table 2. The results indicate that the plastic deformation of the damper of samples AYD-I and AYD-II is higher, and also, there is a possibility that the damper will not yield in the structure. Moreover, it is observed that in general, sample AYD-III has better performance characteristics compared to other samples, and its specific energy absorption and ductility are 261.6 J/kg and 64, respectively. Hence, it can be stated that this member can delay the buckling time of the brace with its ductile behavior so that the damper can absorb a large amount of earthquake input energy without buckling.

Table 3 presents a comparison of key mechanical properties—such as maximum displacement, ductility, total absorbed energy, and damper mass—for the AYD-III auxetic dampers and various metal dampers from previous studies. The auxetic dampers generally demonstrate favorable performance characteristics compared to conventional metal yield dampers. Notably, these auxetic dampers exhibit high ductility, approximately 64, surpassing that of several metal dampers. Additionally, the auxetic damper under investigation offers superior energy absorption, making it a viable alternative to traditional metal yield dampers like ADAS and TADAS.

The auxetic structure employed in the proposed AYM damper offers unique advantages due to its NPR properties, which enhance energy dissipation and deformation characteristics. Unlike conventional materials with a positive Poisson's ratio, auxetic materials expand laterally when stretched and contract when compressed, leading to enhanced deformation under tensile loads. This behavior allows the damper to achieve greater plastic deformation and energy dissipation capacity

Table 3
Comparison of the performance characteristics of an auxetic damper and some common metal yield dampers.

Parameter	Metal yield damper type						
	Auxetic damper (AYD-III)	DPD[a][36]	TADAS[b][37]	SD[c][10]	SPD[d][38]	ShPD[e][39]	SDRDs[f][13]
Construction cost	Low	Very low	High	Low	Very low	Low	high
Ductility	64	36	29	12	-	16	6.7 –13.3
Total dissipated energy (kJ/kg)	261.2	22.7 –49.2	N/A*	6.9 –10.3	-	5.8	158 –228
Height (mm)	640	110 –140	304	162	114 –140	105	860
Mass (kg)	3.8	2.1 –66	95.8	3.1	0.7 –1.0	1.6	13.9

* N/A: Not Available,
[a] Dual-pipe damper,
[b] Triangular-plate added damping and stiffness,
[c] Slit damper,
[d] Single pipe damper,
[e] Shear-panel damper,
[f] Steel dual-ring dampers.

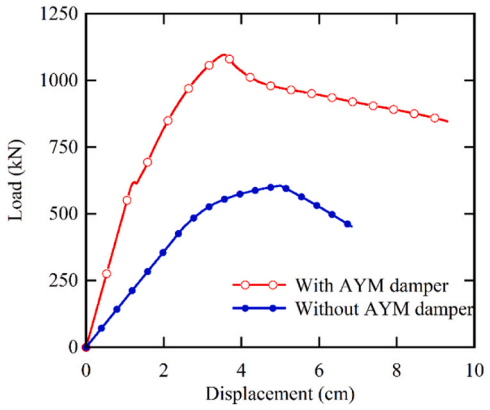

Fig. 9. Influence of the auxetic damper on the load-displacement curve of the steel frame.

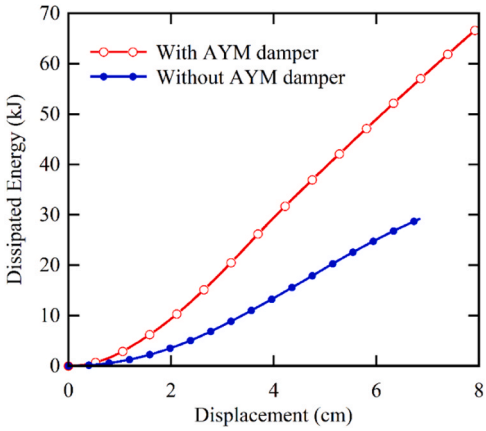

Fig. 10. Dissipated energy curve of the steel frame.

compared to non-auxetic dampers. In this study, samples with a NPR, particularly sample III, demonstrated a higher initial yield force, stiffness, and energy dissipation capability than samples with a positive Poisson's ratio, as shown in Figs. 7 and 8. For example, the auxetic design of sample III achieved a yield force of 21.5 kN, with specific energy absorption reaching 261.2 J/kg and ductility at 64, which are considerably higher than those of conventional designs. These characteristics make the NPR structure advantageous for seismic energy dissipation, as the auxetic structure not only delays buckling but also sustains high levels of deformation without catastrophic failure. The NPR structure also benefits from geometric nonlinearity, which contributes to progressive energy dissipation under large displacements. As illustrated in Fig. 8b, the auxetic sample III maintains resistance at displacements beyond 2 cm due to the interplay of strain stiffening and auxetic deformation, resulting in effective dissipation of seismic energy through repeated plastic deformations. This attribute, combined with the damper's high ductility, allows it to absorb large amounts of input energy, thereby enhancing the resilience of the braced frame under seismic loading. Consequently, the NPR characteristic of the auxetic structure is a crucial factor in achieving high energy dissipation and load-bearing capacity, positioning it as a viable alternative to traditional metal dampers.

However, it is important to acknowledge that these advantages are contingent upon carefully selected geometric configurations. Deviations from the optimal parameters may lead to reduced energy dissipation capacity, lower stiffness, or increased susceptibility to instability and buckling under seismic loading. Therefore, in practical engineering design, it is crucial to tailor the damper's geometry to the specific requirements of the structure and the expected seismic demands. The application prospects of the proposed damper are promising, especially for structures requiring high ductility and energy dissipation capabilities, such as high-rise buildings and bridges in seismic regions. Nonetheless, there are limitations to consider. The fabrication of complex auxetic geometries may present manufacturing challenges, potentially increasing production costs. Additionally, integrating the damper into existing structural systems necessitates careful consideration of connection details, material compatibility, and overall structural dynamics.

6.2. *Steel frame with the proposed damper*

This section examines the effect of the proposed auxetic metallic yield damper on the performance of a steel frame. Displacement-load diagram due to pushover nonlinear static analysis of structures contains valuable information. Therefore, Figs. 9 and 10 illustrates the displacement-load curve and the energy dissipated for the steel frame, respectively. Comparing load-displacement diagrams of structures with dampers and without dampers shows that the suggested auxetic damper possesses a substantial effect on fostering the performance of steel frames. The results indicate that the proposed damper remarkably raises the elastic stiffness, ductility, and energy absorption of the structure. Examination Fig. 9, it can be inferred that the yield strength and ductility of the frame with auxetic damper rise approximately by 136 % and 17 % compared to the frame without damper, respectively.

Another striking point is that in most conventional structures, increasing stiffness almost reduces ductility; however, both stiffness and ductility parameters increase in the proposed system. To confirm this, the ductility value can be calculated according to Fig. 9, which shows that the auxetic damper increases the ductility of the frame understudy from 2.2 to 2.6. According to Fig. 10, which reveals the amount of

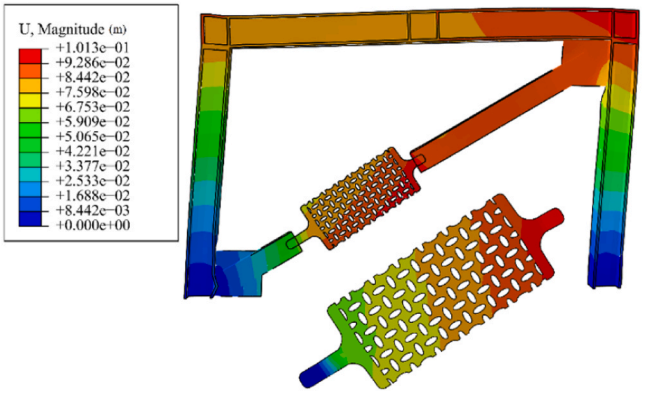

Fig. 11. Deformation of a steel frame equipped with the proposed AYM damper.

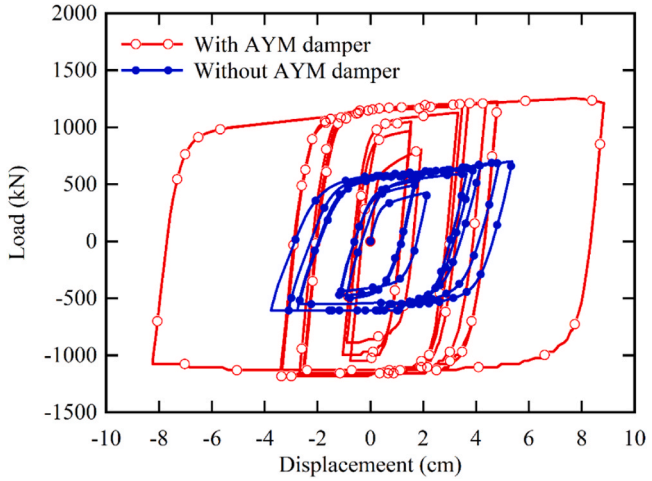

Fig. 12. Comparison of hysteresis curve between steel frames equipped with recommended AYM damper and without damper.

energy dissipated for the braced steel frame, with and without the proposed auxetic damper, it can be observed that the proposed damper significantly enhances energy dissipation and increases energy absorption by nearly three times, which is a considerable number and is much larger as opposed to the existing metal yield dampers' samples. Furthermore, the deformation results in this frame, as provided in Fig. 11, demonstrate that no out-plane deformation was observed in this frame during loading for either the frame or the damper due to the installation of an auxetic damper.

Fig. 12 provides the hysteresis curve of two samples of steel frames with and without proposed AYM dampers. As observed, the hysteresis curve of the frame with the damper is quite stable and indicates the proper performance of the steel frame, including the suggested auxetic damper. According to the results, the frame with the proposed auxetic damper has withstood almost three times its yield displacement cycle. Furthermore, the presence of dampers in this frame has increased the initial stiffness of the frame significantly. It should be noted that at the end of the applied load, there was no sign of cracking in the damper or a decrease in strength and stiffness in its hysteresis curve, and the damper was still able to withstand more load cycles. The hysteresis curve of the structures equipped with this type of damper is without reducing stiffness and resistance decline, and narrowing does not occur in them. These dampers increase the stiffness of the structure before failure occurs. Therefore the seismic performance is improved by adding the proposed brace system and the proposed AYM damper to the bending frames. These results, once again, confirm the possibility of utilizing the

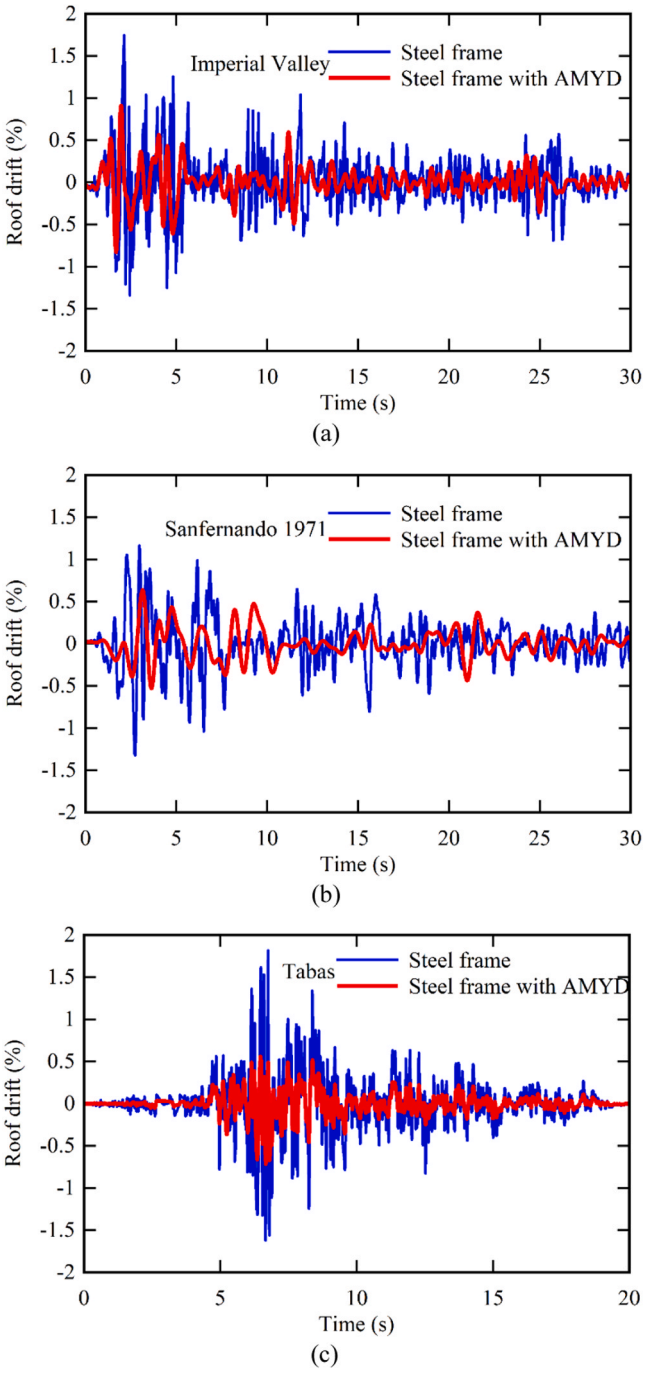

Fig. 13. Roof drift for 10-story steel frame with and without AMY damper for 3 earthquake records, (a) Imperial Valley, (b) Sanfernando, and (c) Tabas.

proposed auxetic damper in structures as an energy dissipater.

These types of dampers with nonlinear behavior prevent any damage caused by nonlinear behavior in the main and secondary components of the structure. Consequently, the metal we choose for this type of dampers should have high hardness, high fatigue cycle, and insensitivity to temperature changes, high relative strength, and appropriate behavior to change hysteresis. Selecting the proper material and appropriate geometry of the metal applied, and the correct location of these dampers will increase the structure's life and increase the life and durability of the dampers themselves.

To assess the impact of the new damper on the seismic behavior of high-rise buildings, the response of a 10-story steel frame equipped with the proposed AYM damper is thoroughly analyzed. Fig. 13 present the

Table 4
Maximum base shear, displacement and roof acceleration of the models with and without AYM dampers under 3 earthquake records.

Ground motion	Max. base shear (kN)		Max. displacement (cm)		Max. roof acceleration (m/s^2)	
	Normal brace	Brace with AYM damper	Normal brace	Brace with AYM damper	Normal brace	Brace with AYM damper
Imperial Valley	8650	5970	36.85	22.85	5.36	2.17
Sanfernando 1971	6284	4308	31.08	18.94	4.08	2.36
Tabas 1978	10,560	6850	44.92	15.49	10.68	4.85

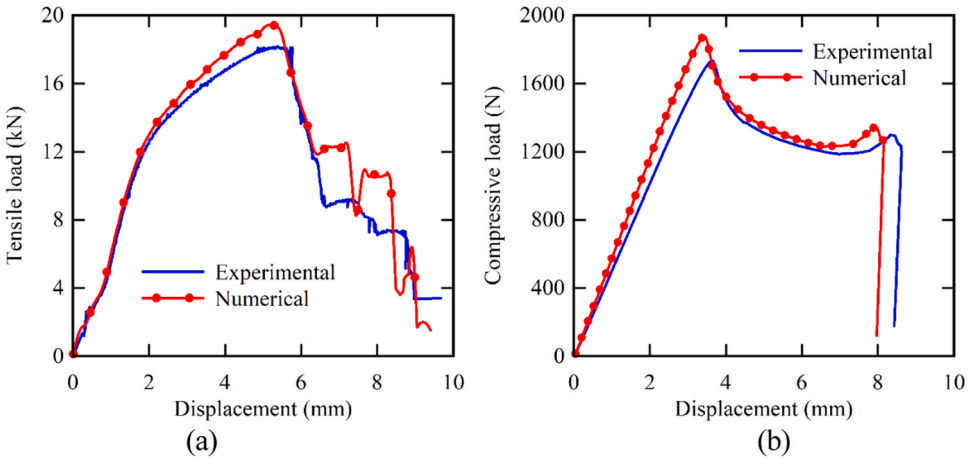

Fig. 14. Comparison of numerical and experimental results for AYN damper (a) load-displacement for tensile loading condition, and (b) compressive loading condition.

roof drift (%) for the evaluated seismic ground motions. The peak roof drift, which affect the usability of housing, were significantly lower for the steel frame with proposed dampers than for the steel frame without dampers. The maximum drift observed during the Tabas earthquake for the steel frame without the damper and with the damper is approximately 1.82 g and 0.56 g, respectively, demonstrating a 225 % improvement in drift reduction with the incorporation of the proposed AMY damper. Table 4 show the maximum displacement, base shear and roof acceleration. It sounds that damper influences in reducing the base shear and maximum displacement are more than that in acceleration. The results indicate that incorporating AYM dampers significantly enhances the seismic performance of the structure across all evaluated metrics. Maximum base shear is reduced by approximately 31–35 %, with values dropping from 8650 kN to 5970 kN for the Imperial Valley earthquake, 6284 kN to 4308 kN for San Fernando, and 10,560 kN to 6850 kN for Tabas. Similarly, maximum displacement decreases by around 36–39 %, improving from 36.85 cm to 22.85 cm under Imperial Valley, 31.08 cm to 18.94 cm for San Fernando, and 44.92 cm to 28.49 cm during Tabas. Roof acceleration also shows a substantial reduction, with decreases of 47–55 %, as seen in the drop from 5.36 m/s^2 to 2.17 m/s^2 for Imperial Valley, 4.08 m/s^2 to 2.36 m/s^2 for San Fernando, and 10.68 m/s^2 to 4.85 m/s^2 for Tabas. These reductions highlight the AYM damper's effectiveness in enhancing structural stability and mitigating seismic forces.

7. Validation of the numerical model

The numerical results for the AYM damper were validated through comparison with experimental data obtained using a universal testing machine under both tensile and compressive loading conditions. By comparing load-displacement responses, the validity of the model was established. Fig. 14 illustrates the comparison between the experimental and numerical load-displacement and energy-displacement responses for AYM damper under quasi-static tensile and compressive load, respectively. In conclusion, it is clear from the numerical results that they are generally in agreement with the ultimate load, with a slight overprediction at the end of the deformation process. This overprediction is attributed to the stress-strain curve of the material used in this study, which exhibits an unusual strain-softening phenomenon characterized by a negative slope. The bilinear material prediction model cannot account for this material behavior because it requires a slope greater than zero between the data points. Consequently, it is possible that the finite element model is not capable of capturing the material strain softening phenomenon with sufficient accuracy. Table 5 illustrates the comparison of experimental and predicted values of SEA and ultimate force. From this table, it is evident that the percentage of errors is within acceptable limits. According to Table 5 and Fig. 14, there is a good correlation between the numerical and experimental results. Fig. 14 illustrates a close correlation between the predicted deformation modes and those observed during experimental testing for an auxetic damper under quasi-static tensile loading. Similar to the numerical model, the width of the middle area of the damper increased during the deformation of the experimental sample. This indicates the auxetic behavior of the proposed metallic yield damper.

The results reveal that the compressive bearing capacity of the model-C sample, obtained through experimental testing and finite element analysis, is 1722 N and 1866 N, respectively. This indicates that the FEA model's compression analysis predicts values approximately 8.4 % higher than the experimental results. This variation may stem from geometric imperfections and non-ideal boundary conditions present in the experimental setup, which the finite element model may not fully capture. Consequently, the FEA model provides a slightly conservative estimate, making it practical for predictive purposes. In the auxetic structure, the unique cellular configuration ensures that compressive strength does not immediately drop to zero upon buckling. Instead, the compressive strength initially declines modestly, followed by a recovery as the structure progresses along the post-buckling path. This pattern reflects the inherent stability provided by the auxetic design, allowing the structure to resist collapse at initial stages of buckling. Eventually, as the compressive load continues to increase, the damper experiences significant buckling around a displacement of 8 mm, which results in a rapid and pronounced loss of strength. This

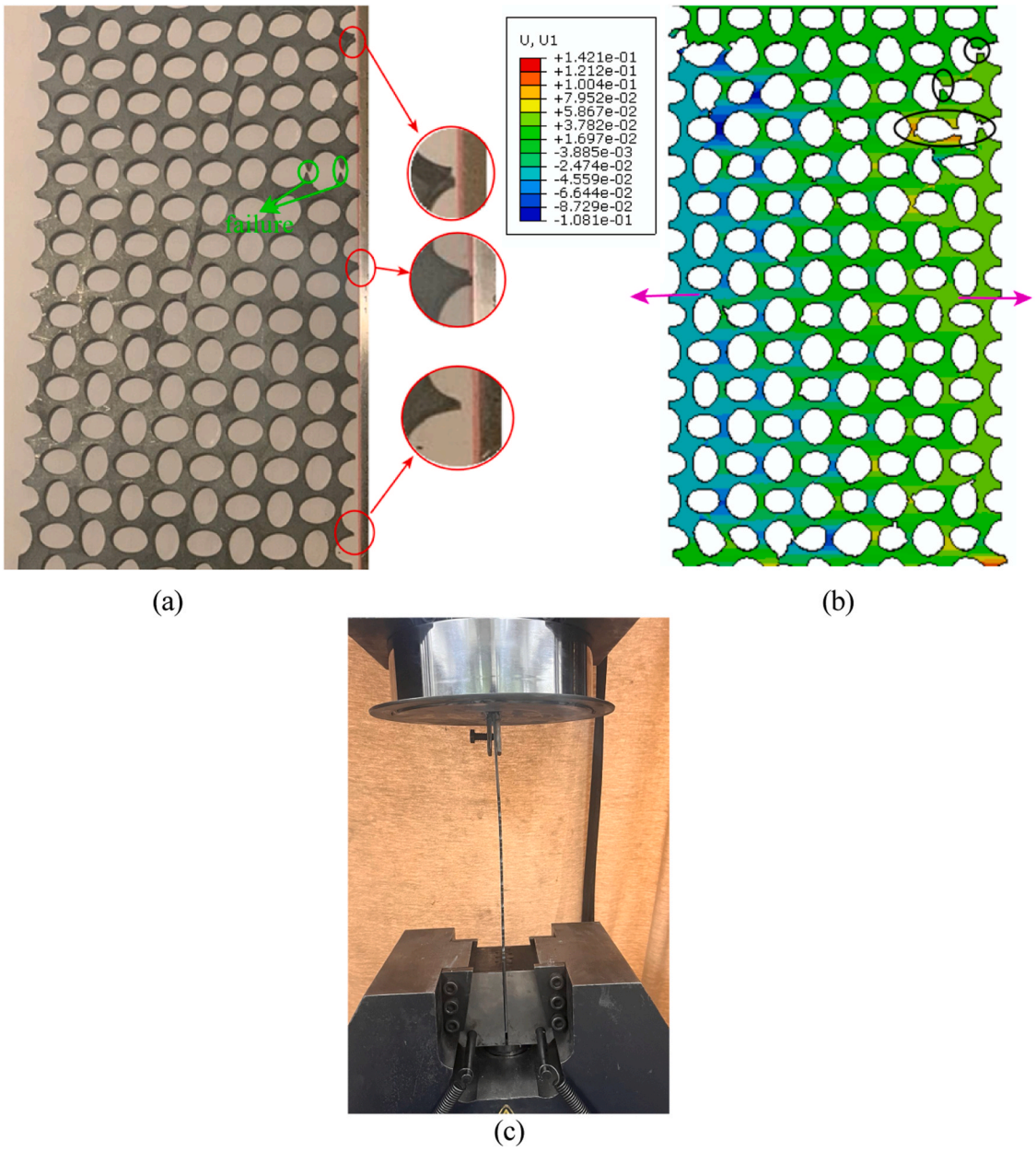

Fig. 15. Comparison of (a) the experimental, (b) the numerical deformation of AYM damper under quasi-static tensile loading, (c) buckling deformation under quasi-static compressive loading.

Table 5
Comparison of numerical and experimental results for AYM damper.

	SEA [j/kg]	Ultimate tensile load [kN]	Ultimate compressive load [N]
Experimental	104.56	18.14	1722
Numerical	111.67	19.37	1866
Error (%)	6.8	6.7	8.4

progressive post-buckling behavior, coupled with the auxetic structure's resilience, underscores its ability to sustain load through controlled deformation before reaching a critical failure point. Fig. 14c illustrates the deformation behavior of this sample under compressive loading, highlighting the gradual structural response prior to full buckling.

This study demonstrates the potential of the auxetic metallic yield damper, with its negative Poisson's ratio structure, to improve seismic energy dissipation and deformation capacity. The auxetic design allows the damper to withstand both tensile and compressive forces, enhancing plastic deformation and energy dissipation. However, we acknowledge that additional critical investigations are necessary to comprehensively understand the damper's performance under realistic seismic conditions. Future research should focus on in-depth cyclic performance testing to evaluate the damper's long-term behavior under repeated loading conditions. This includes detailed studies on the effect of different boundary conditions, which can significantly influence the damper's stability and energy dissipation. Furthermore, exploring variations in the geometrical design, such as adjusting hole sizes, orientations, and the overall auxetic pattern, could optimize the damper's performance, particularly in high-seismic-demand scenarios. Advanced modeling and experimental studies are also recommended to validate and extend the findings of this study, providing a stronger foundation for the use of auxetic structures in earthquake engineering applications. These additional investigations will provide more profound insights into the structural resilience of auxetic dampers, supporting their potential

integration into seismic design strategies and high-performance structural systems.

8. Conclusion

A new AYM damper is introduced in this paper, comprising a steel plate with elliptical holes with proper distribution and NPR. The primary purpose is to increase the seismic performance of the frame, increase ductility, stiffness, and damage control in the frame. In order to demonstrate the auxetic effect of the present design and simultaneously verify the computational model, experiments and finite element simulations of uniaxial tensile and compressive tests are carried out on the specific sample. The proposed auxetic damper is attached to the braced frame as a diagonal brace and prevents the nonlinear behavior of the frame by plastic yielding and acting as a ductile fuse. Taking into consideration the finite element analyses conducted, a summary of the results of the present study can be summarized as follows:

- The samples with regular and uniform holes own a positive Poisson's ratio and non-auxetic behavior.
- By applying tension load, the middle part of the samples undergoes a reduction in length and shrinkage. Furthermore, increasing the volume fraction of holes and the use of elliptical holes with non-uniform distribution raises the auxetic feature of the structure.
- The proposed AYM damper specific absorbed energy and ductility are 57.6 J/kg and 64, respectively. Dissipated energy due to plastic yield and deformation indicates the high ability of auxetic dampers in energy dissipation.
- Another importance of the new AYM damper is its high ductility, which is about 64 and is considerably higher than the ductility of various commercial metal dampers.
- The proposed AYM damper raises the ductility of the steel frame from 2.2 to 2.6. Also, the proposed auxetic damper substantially improves energy dissipation by virtually 3 times, which is a remarkable and is a lot larger than the existing metallic yield damper models.
- The hysteresis curve of the frame equipped with the proposed AYM damper is quite stable and demonstrates the proper performance of the system. Additionally, the presence of dampers in this frame has raised the initial stiffness of the frame dramatically.

Comparing some of the performance characteristics of the proposed dampers with some of the existing metal yield dampers confirms that the auxetic dampers proposed can generally outperform the prevalent AYM dampers. These results, once again, verify the probability of applying the proposed auxetic damper in structures as an energy dissipater. Considering these factors, the proposed damper shows promise for earthquake-resistant structures, particularly in applications where high energy dissipation and durability are crucial. However, its use in practice will require careful design and testing to ensure its performance under a range of loading conditions and environmental factors.

This study demonstrates the effectiveness of the AYM damper in enhancing seismic performance metrics, including energy dissipation, base shear reduction, and displacement control. While this research successfully evaluates the damper's behavior under specific loading conditions, future testing under compressive and low cycle hysteresis conditions will require strategies to mitigate potential instability.

CRediT authorship contribution statement

Majid Pouraminian: Investigation, Methodology. **Ahmed Genjaly:** Project administration, Resources, Supervision, Writing – original draft. **Hakan Çağlar:** Investigation, Methodology, Writing – review & editing, Software. **Saeed Lari:** Data curation, Formal analysis, Software, Validation. **Mehrdad Ashtari:** Validation, Writing – review & editing. **Rohollah Salmani:** Investigation, Methodology, Writing – original draft.

Declaration of Competing Interest

The authors hereby report no conflicts of interest with regards to this work.

References

[1] Rezaee M, Maleki VArab. Passive vibration control of fluid conveying pipes using dynamic vibration absorber. Amirkabir J Mech Eng 2019;51(3):111–20.
[2] Nasrabadi M, Sevbitov AV, Maleki VA, Akbar N, Javanshir I. Passive fluid-induced vibration control of viscoelastic cylinder using nonlinear energy sink. Mar Struct 2022;81:103116.
[3] Addala MB, Bhalla S, Madan A. Performance based design of a new hybrid passive energy dissipation device for vibration control of reinforced concrete frames subjected to broad-ranging earthquake ground excitations. Adv Struct Eng 2022;25(4):895–912.
[4] Rezaee M, Maleki VArab. Vibration characteristics of fluid-conveying pipes in presence of a dynamic vibration absorber. Modares Mech Eng 2017;17(7):31–8.
[5] Khosravi S, Amjadian M. A parametric study on the energy dissipation capability of frictional mechanical metamaterials engineered for vibration isolation. in *Active and Passive Smart Structures and Integrated Systems XVIII*. SPIE,; 2024.
[6] Li G, Zhu L-H, Li H-N. Displacement-based seismic design for buildings installed hysteretic dampers with hardening post-yielding stiffness. Adv Struct Eng 2019;22(16):3420–34.
[7] Gur S, Xie Y, DesRoches R. Seismic fragility analyses of steel building frames installed with superelastic shape memory alloy dampers: comparison with yielding dampers. J Intell Mater Syst Struct 2019;30(18-19):2670–87.
[8] Mohammadi RK, Nasri A, Ghaffary A. TADAS dampers in very large deformations. Int J Steel Struct 2017;17(2):515–24.
[9] Maleki S, Mahjoubi S. Infilled-pipe damper. J Constr Steel Res 2014;98:45–58.
[10] Chan RW, Albermani F. Experimental study of steel slit damper for passive energy dissipation. Eng Struct 2008;30(4):1058–66.
[11] Balendra T, Yu CH, Lee FL. An economical structural system for wind and earthquake loads. Eng Struct 2001;23(5):491–501.
[12] Downey A, Theisen C, Murphy H, Anastasi N, Laflamme S. Cam-based passive variable friction device for structural control. Eng Struct 2019;188:430–9.
[13] Azandariani MG, Azandariani AG, Abdolmaleki H. Cyclic behavior of an energy dissipation system with steel dual-ring dampers (SDRDs). J Constr Steel Res 2020;172:106145.
[14] Guo W, Ma C, Yu Y, Bu D, Zeng C. Performance and optimum design of replaceable steel strips in an innovative metallic damper. Eng Struct 2020;205:110118.
[15] Guo W, Wang X, Yu Y, Chen X, Li S, Fang W, et al. Experimental study of a steel damper with X-shaped welded pipe halves. J Constr Steel Res 2020;170:106087.
[16] Lu Z, Yang Y, Lu X, Liu C. Preliminary study on the damping effect of a lateral damping buffer under a debris flow load. Appl Sci 2017;7(2):201.
[17] Zhao N, Lu C, Chen M, Luo N, Liu C. Parametric study of pounding tuned mass damper based on experiment of vibration control of a traffic signal structure. J Aerosp Eng 2018;31(6):04018108.
[18] Lim T-C. Auxetic materials and structures, 2779. Springer,; 2015.
[19] Lakes R. Foam structures with a negative poisson's ratio. Science 1987;235(4792):1038–40.
[20] Zhang J, Lu G, You Z. Large deformation and energy absorption of additively manufactured auxetic materials and structures: a review. Compos Part B: Eng 2020;201:108340.
[21] Meena K, Singamneni S. A new auxetic structure with significantly reduced stress concentration effects. Mater Des 2019;173:107779.
[22] Ren X, Shen J, Ghaedizadeh A, Tian H, Xie YM. A simple auxetic tubular structure with tuneable mechanical properties. Smart Mater Struct 2016;25(6):065012.
[23] Hassanin H, Abena A, Elsayed MA, Essa K. 4D printing of NiTi auxetic structure with improved ballistic performance. Micromachines 2020;11(8):745.
[24] Guo Y, Zhang J, Chen L, Du B, Liu H, Chen L, et al. Deformation behaviors and energy absorption of auxetic lattice cylindrical structures under axial crushing load. Aerosp Sci Technol 2020;98:105662.
[25] Nedoushan RJ, Yu W-R. A new auxetic structure with enhanced stiffness via stiffened elliptical perforations. Funct Compos Struct 2020;2(4):045006.
[26] Peixinho N, Carvalho O, Areias C, Pinto P, Silva F. Compressive properties and energy absorption of metal-polymer hybrid cellular structures. Mater Sci Eng: A 2020;794:139921.
[27] Lolaki A, Zarrebini M, Mostofinejad D, Shanbeh M, Abtahi SM. Intensification of auxetic effect in high stiffness auxetic yarns with potential application as the reinforcing element of composite. J Ind Text 2020:1528083720978918.
[28] Behravanrad A, Jafari M. Thermoporoelasticity analysis of variable thickness and elastically restrained functionally graded auxetic metamaterial circular plate resting on an auxetic material circular plate. Proc Inst Mech Eng Part C J Mech Eng Sci 2020;235(16):3036–57.
[29] Bae J, Huang X, Zhang Z. Advanced seismic resilient performance of steel MRF equipped with viscoelastic friction dampers. Sci Rep 2024;14(1):19403.
[30] Khosravi S, Goudarzi MA. Seismic risk assessment of on-ground concrete cylindrical water tanks. Innov Infrastruct Solut 2023;8(1):68.
[31] Alizadeh Aa, Sarvestani FS, Zekri H, AL-Khafaji MO, Salman HM, Ganji DD, et al. The novelty of using the AGM and FEM for solutions of partial differential and

ordinary equations along a stretchable straight cylinder. Case Stud Therm Eng 2023;45:102946.
[32] An Q, Bagheritabar M, Basem A, Ghabra AA, Li Y, Tang M, et al. The effect of size of copper oxide nanoparticles on the thermal behavior of silica aerogel/paraffin nanostructure in a duct using molecular dynamics simulation. Case Stud Therm Eng 2024;60:104666.
[33] Emami F, Kabir MZ. Performance of composite metal deck slabs under impact loading. Structures 2019;19:476–89.
[34] Krawinkler H. Cyclic loading histories for seismic experimentation on structural components. Earthq Spectra 1996;12(1):1–12.
[35] Mohebkhah A, Azandariani MG. Lateral-torsional buckling resistance of unstiffened slender-web plate girders under moment gradient. Thin-Walled Struct 2016;102:215–21.
[36] Maleki S, Mahjoubi S. Dual-pipe damper. J Constr Steel Res 2013;85:81–91.
[37] Tsai K-C, Chen H-W, Hong C-P, Su Y-F. Design of steel triangular plate energy absorbers for seismic-resistant construction. Earthq Spectra 1993;9(3):505–28.
[38] Maleki S, Bagheri S. Pipe damper, part I: experimental and analytical study. J Constr Steel Res 2010;66(8-9):1088–95.
[39] Li Z, Albermani F, Chan RW, Kitipornchai S. Pinching hysteretic response of yielding shear panel device. Eng Struct 2011;33(3):993–1000.